Systematic calculations of low-lying states of even-even nuclei within the nucleon pair approximation

L. Y. Jia,[1,2] H. Zhang,[1,3] and Y. M. Zhao[1,4,5,6,*]

[1]*Department of Physics, Shanghai Jiao Tong University, Shanghai 200240, People's Republic of China*

[2]*Department of Electric and Information Engineering, Shanghai Jiao Tong University, Shanghai 200240, People's Republic of China*

[3]*Department of Biology, Shanghai Jiao Tong University, Shanghai 200240, People's Republic of China*

[4]*Cyclotron Center, Institute of Physical Chemical Research (RIKEN), Hirosawa 2-1, Wako-shi, Saitama 351-0198, Japan*

[5]*Center of Theoretical Nuclear Physics, National Laboratory of Heavy Ion Accelerator, Lanzhou 730000, People's Republic of China*

[6]*CCAST, World Laboratory, P. O. Box 8730, Beijing 100080, People's Republic of China*

(Received 23 October 2006; published 16 March 2007)

A collective S and D nucleon pair approximation of the shell model is applied to even-even Sn, Te, Xe, Ba, and Ce isotopes with mass number $A \sim 120$–150 and neutron number ranging from 74 to 90. Our Hamiltonian employs monopole pairing, quadrupole pairing plus quadrupole-quadrupole-type interactions between like valence nucleons and quadrupole-quadrupole interactions between valence neutrons and valence protons. With very few parameters, the low-lying states of even-even Sn, Te, Xe, Ba, and Ce isotopes are well described. The calculated $B(E2)$ values and g factors are consistent with recent experimental data. Our systematic calculations also predict $B(E2)$ values and g factors (in particular, for nuclei with valence neutrons in the 82–126 region) if these data are not available.

DOI: 10.1103/PhysRevC.75.034307 PACS number(s): 21.10.Re, 21.60.Ev, 21.60.Cs, 27.60.+j

I. INTRODUCTION

One of the central problems of nuclear structure theory is to describe the collective and low-lying excitations in terms of the spherical shell model. Because the shell-model configuration space for medium and heavy nuclei is usually prohibitively huge, one needs to select collective configurations from the whole shell-model space. Through the great success of the interacting boson model (IBM) [1], it has been generally recognized that the collective pairs with spin zero (S) and spin two (D) play a dominant role in collective motions of low-lying states for medium and heavy nuclei. The IBM stimulated many studies of collectivity by using correlated S pairs and D pairs as building blocks of the model space, e.g., the fermion dynamical symmetry model (FDSM) [2], the broken pair approximation (BPA) [3], the favored pair approximation (FPA) [4], etc.

In 1993 Chen studied the application of Wick theorem to coupled clusters and obtained recursion relations of calculating matrix elements of a Hamiltonian within a multipair basis [5]. Based on this technique, he proposed a nucleon-pair shell model (NPSM) [6]. In the NPSM, nucleon pairs with various angular momenta are used as building blocks of the truncated shell-model space. If one restricts only a few types of collective pairs as building blocks of the model space, the NPSM is called nucleon-pair approximation of the shell model (NPA). The NPA is flexible enough to include the BPA, the FPA, and the FDSM as its special cases, because nucleon pairs in the NPA can be arbitrarily constructed if necessary. A simplified and unified version of the NPA was developed in Ref. [7].

In numerical calculations one usually truncates the shell space to collective SD-pair subspace. Description of some specific states may need other pairs. For example, one needs G pairs in deformed regions [8]; one needs one pair with spin equal to 10 (alignment of two particles in $h_{11/2}$ orbit) to improve the description of spin 6–10 states of the yrast band of even-even ^{132}Ba [9]. However, for low excitations the SD-pair truncation is reasonably good when the deformation of nuclei is not so large, which is the case for nuclei discussed in this work.

In this article, we apply the SD version of the NPA to Sn, Te, Xe, Ba, and Ce isotopes, with neutron number ranging from 74 to 90. Although there were a number of calculations on Sn, Te, Xe, Ba, and Ce isotopes with both valence protons and valence neutrons (holes) in the 50–82 shell, there have been few systematic and microscopic calculations of low-lying states with valance neutrons in the 82–126 shell for these isotopes, except quantum Monte Carlo shell-model calculations on Te isotopes by Shimizu *et al.* in Ref. [10], shell-model calculations on some Xe, Te isotopes by Jakob *et al.* in Ref. [11], and on some Sn, Te, Xe isotopes by Brown *et al.* in Ref. [12], where those authors calculated systems with only a very few valence neutrons outside the $N = 82$ shell. In this article we shall calculate cases with more valence neutrons in the 82–126 shell by using our nucleon pair approximation.

This article is organized as follows. In Sec. II we give a brief introduction of our formulation, which includes our pair configuration basis, Hamiltonian, and transition operators. In Sec. III we discuss the pair structure coefficients and Hamiltonian parameters used in this article. In Sec. IV our calculated results are presented and compared with experimental data. In Sec. V we summarize our calculated results and conclusions of this article.

*Corresponding author. Electronic address: ymzhao@sjtu.edu.cn

II. FRAMEWORK OF OUR CALCULATIONS

A collective pair of spin r and projection μ is defined by

$$A^{r\dagger}_{\mu} = \sum_{ab} y(abr)(C^{\dagger}_{a} \times C^{\dagger}_{b})^{r}_{\mu}. \tag{1}$$

The a, b denote all quantum numbers (except the magnetic quantum number) necessary to specify a state $[a \equiv (nlj)]$. We also use them to denote the spin j of the single-particle orbit. The $C^{\dagger}_{a}$ and $C^{\dagger}_{b}$ are single-particle creation operators. $r = 0$ and 2 correspond to S pair and D pair, respectively. One easily sees that structure coefficients $y(abr)$ follow the symmetry

$$y(abr) = -(-)^{a+b+r} y(bar).$$

The nucleon pairs are coupled stepwise to construct the N-pair basis

$$\begin{aligned} &|\tau J_N M_N\rangle \equiv A^{J_N\dagger}_{M_N}(r_i, J_i)|0\rangle, \\ &A^{J_N\dagger}_{M_N}(r_1 r_2 \ldots r_N, J_1 J_2 \ldots J_N) \\ &\quad = [\ldots (A^{r_1\dagger} \times A^{r_2\dagger})^{J_2} \times \ldots \times A^{r_N\dagger}]^{J_N}_{M_N}, \end{aligned} \tag{2}$$

where $J_1 = r_1$, J_N is the total angular momentum of the N-pair operator, and M_N is the z projection of J_N. Here τ is an abbreviation for all the necessary intermediate quantum numbers. It is noted that for a fixed total number n of S and D pairs the number of linear independent basis states for a given angular momentum J_N is usually equal to that of the sd boson states, with very few finite exceptions, which are Pauli blocked. There are various ways to choose intermediate angular momenta J_i $(i = 2 \cdots N-1)$ to make those basis states. For a given J_N, it would be better to choose the smallest value for each J_i to save computing time. The choice of J_i $(i = 2 \cdots N-1)$ must ensure the basis are linear independent.

The time reversal of the above N-pair operator is

$$\begin{aligned} &\tilde{A}^{J_N}_{M_N}(r_1 r_2 r_3 \ldots r_N, J_1 J_2 J_3 \ldots J_N) \\ &\quad = \left\{ \ldots \left[(\tilde{A}^{r_1} \times \tilde{A}^{r_2})^{J_2} \times \tilde{A}^{r_3} \right]^{J_3} \times \cdots \times \tilde{A}^{r_N} \right\}^{J_N}_{M_N} \\ &\quad \equiv \tilde{A}^{J_N}_{M_N}(r_i, J_i). \end{aligned} \tag{3}$$

The $\tilde{A}^{r_i}$ is defined as

$$\tilde{A}^{r_i} = (-) \sum_{ab} y(abr_i)(\tilde{C}_a \times \tilde{C}_b)^{r_i},$$

where $\tilde{C}_{am} = \tilde{C}_{(nlj)m} = (-)^{j-m} C_{a-m}$, and C_{am} is the annihilation operator.

In this article the Hamiltonian is defined as follows.

$$H = H_0 + H_P + \kappa Q_\pi \cdot Q_\nu. \tag{4}$$

The first part is the spherical single-particle energy term,

$$H_0 = \sum_{\alpha\sigma} \epsilon_{\alpha\sigma} C^{\dagger}_{\alpha\sigma} C_{\alpha\sigma}, \tag{5}$$

where α denotes all quantum numbers necessary to specify a state, $\alpha \equiv (nljm)$, and $\sigma = \pi, \nu$ corresponds to degree of freedom for protons and neutrons, respectively.

The second term is residual interaction between like valence particles and is assumed to consist of monopole and quadrupole pairing and quadrupole-quadrupole interactions:

$$H_P = V_0 + V_2 + V_Q, \tag{6}$$

where V_0 is monopole pairing interaction

$$V_0 = G_\pi \mathcal{P}^{\dagger}_{\pi} \mathcal{P}_\pi + G_\nu \mathcal{P}^{\dagger}_{\nu} \mathcal{P}_\nu, \tag{7}$$

where

$$\mathcal{P}^{\dagger}_{\sigma} = \sum_{a_\sigma} \frac{\hat{j}_\sigma}{2} \left(C^{\dagger}_{a_\sigma} \times C^{\dagger}_{a_\sigma}\right)^{0}_{0},$$

with $\hat{j} = (2j+1)^{\frac{1}{2}}$. The V_2 in Eq. (6) is quadrupole pairing force defined as follows.

$$V_2 = \sum_{\sigma} G^2_\sigma \mathcal{P}^{(2)\dagger}_{\sigma} \cdot \mathcal{P}^{(2)}_{\sigma}, \tag{8}$$

where $\mathcal{P}^{(2)\dagger}_{\sigma}$ is defined as

$$\mathcal{P}^{(2)\dagger}_{\sigma M} = \sum_{a_\sigma b_\sigma} q(a_\sigma b_\sigma)\left(C^{\dagger}_{a_\sigma} \times C^{\dagger}_{b_\sigma}\right)^{2}_{M},$$

with $M = 0, \pm 1, \pm 2$; $q(a_\sigma b_\sigma)$ is the same as the $q(ab)$ appears in the Q_σ operator

$$Q_M = \sum_{ab} q(ab) \left(C^{\dagger}_{a} \times \tilde{C}_b\right)^{2}_{M}, \tag{9}$$

with $q(ab) = \frac{(-)^{j_a - 1/2}}{\sqrt{20\pi}} \hat{j}\hat{j}' C^{20}_{j1/2, j'-1/2} \langle nl|r^2|nl'\rangle$. Here $C^{20}_{j1/2, j'-1/2}$ is the Clebsch-Gordan coefficient. The matrix elements of r^2 are given in Ref. [13].

$$\begin{aligned} &\langle nl|r^2|nl'\rangle \\ &\quad = \begin{cases} (n + 3/2) {r_0}^2 & l = l', \\ (n + l' + 2 \pm 1)^{1/2} (n - l' + 1 \mp 1)^{1/2} {r_0}^2 & l = l' \pm 2, \end{cases} \end{aligned}$$

where ${r_0}^2 = \frac{\hbar}{M_N \omega_0} = 1.012 A^{1/3} fm^2$. M_N is mass of a nucleon, and ω_0 is the harmonic oscillator frequency. Note that the script $\sigma = \pi$ or ν is omitted in the above definition because Q is just $r^2 Y^2_M$, and it has the same form for protons and neutrons. We do not use the actual value of ${r_0}^2$ when we calculate the excitation energies and binding energies in this article, because quadrupole pairing and quadrupole interaction strengths are given in unit of MeV/${r_0}^4$.

The V_Q in Eq. (6) is quadrupole-quadrupole interaction between like valence nucleon,

$$V_Q = \sum_{\sigma} \kappa_\sigma Q_\sigma \cdot Q_\sigma. \tag{10}$$

The $E2$ transition operator is

$$T(E2) = e_\pi Q_\pi + e_\nu Q_\nu, \tag{11}$$

where e_ν and e_π are effective charges of valence neutrons and protons that include their bare charges, respectively. The $B(E2)$ value is given by

$$B(E2) = \frac{2J_f + 1}{2J_i + 1} \langle T(E2)\rangle^2, \tag{12}$$

where J_f, J_i stands for the angular momentum of the final state, initial state, respectively.

TABLE I. Single-particle energies taken in this article. The upper table presents single-particle energies for both valence protons (particle-like) and valence neutrons (hole-like) in the 50–82 shell. The lower table lists single-particle energies of valence neutrons for the same isotopes with valence neutrons (particle-like) in the 82–126 shell. Taken from Refs. [15–17].

j	$s_{1/2}$	$d_{3/2}$	$d_{5/2}$	$g_{7/2}$	$h_{11/2}$	
ϵ_π(MeV)	2.990	2.690	0.963	0	2.76	
ϵ_ν(MeV)	0.332	0.000	1.655	2.434	0.242	
j	$p_{1/2}$	$p_{3/2}$	$f_{5/2}$	$f_{7/2}$	$h_{9/2}$	$i_{13/2}$
ϵ_ν(MeV)	1.656	0.854	2.005	0.000	1.561	1.800

The magnetic moment operator is

$$\mu = g_{l\pi} L_\pi + g_{l\nu} L_\nu + g_{s\pi} S_\pi + g_{s\nu} S_\nu, \tag{13}$$

where π and ν represent proton and neutron degree of freedom, respectively. g_l and g_s are the orbital and spin gyromagnetic ratios. The total orbital angular momentum operator L and total spin S can be identified with collective dipole operators as below:

$$L_\sigma = Q^1_{l\sigma} = \sum_{ab} q_l(ab1)(C^\dagger_a \times \tilde{C}_b)^1, \qquad \sigma = (\pi, \nu),$$

$$S_\sigma = Q^1_{s\sigma} = \sum_{ab} q_s(ab1)(C^\dagger_a \times \tilde{C}_b)^1, \qquad \sigma = (\pi, \nu),$$

with

$$q_l(ab1) = (-1)^{l+1/2+b} \sqrt{\frac{l(l+1)}{3}} \hat{a}\hat{b}\hat{l} \begin{Bmatrix} a & b & 1 \\ l & l & 1/2 \end{Bmatrix},$$

$$q_s(ab1) = (-1)^{l+1/2+a} \sqrt{\frac{1}{2}} \hat{a}\hat{b} \begin{Bmatrix} a & b & 1 \\ 1/2 & 1/2 & l \end{Bmatrix}.$$

The g factor is defined by μ/J.

There are several computer codes for the NPA calculation. The input includes single-particle energies, the parameters of the Hamiltonian, effective charges in the $E2$ operator, and effective g factors in the magnetic moment operator μ. The output includes calculated energies for low-lying levels, $E2$ and $M1$ transition rates among these states, and so on.

III. PARAMETERS OF THE HAMILTONIAN

Let us discuss first structure coefficients of our S and D pairs. In this article we use the BCS pair as our S pair. For given pairing strengths G_ν and G_π we solve the BCS equation to obtain the empty and occupied amplitude, u_a and v_a. Our S pair is then given by

$$S^\dagger = \sum_a y(aa0)(C^\dagger_a \times C^\dagger_a)^0, \quad y(aa0) = \hat{a}\frac{v_a}{u_a}. \tag{14}$$

The D pair is obtained by using the commutator

$$D^\dagger = \tfrac{1}{2}[Q, S^\dagger] = \sum_{ab} y(ab2)(C^\dagger_a \times C^\dagger_b)^2, \tag{15}$$

as suggested and studied in the references in Ref. [14]. Here operator Q is defined in Eq. (9). From Eq. (15), it is easy to obtain (after symmetrization)

$$y(ab2) = -\frac{1}{2} q(ab) \left[\frac{y(aa0)}{\hat{a}} + \frac{y(bb0)}{\hat{b}} \right]. \tag{16}$$

There are other ways to define S and D pairs [8], but it is expected that the choice of SD-pair structure coefficients given in Eqs. (14) and (16) is one of the best ways when the quadrupole-quadrupole interaction between protons and neutrons are strong. Note that we omitted the script π or ν here because we determine S and D pairs separately for protons and neutrons in the same way and this omission does not cause confusion.

Our neutron single-particle energies of the 50–82 shell are taken from experimental data of Ref. [15] and neutron single-particle energies of the 82–126 shell, and proton single-particle energies are obtained from an extension of available experimental data of Refs. [16] and [17]. These values are given in Table I. By taking these single particle energies, we calculate low-lying states of even-even nuclei with proton number $50 \leqslant Z \leqslant 58$ and neutron number $74 \leqslant N \leqslant 90$.

We next come to parametrization of our phenomenological shell-model Hamiltonian, as given in last section. One of improvements that we made in this work is that we propose a method to determine parameters of the above Hamiltonian for nuclei with both valence protons and valence neutrons outside the core, by introducing two phenomenological requirements that will be explained later. Here let us first exemplify our procedure by cases with both valence neutrons and valence protons in the 50–82 shell. The same procedure is applied to cases with valence protons in the 50–82 shell and valence neutrons in the 82–126 shell.

(i) We fix G_π, G_ν, κ for all these isotopes with valence neutrons in the 50–82 shell. We take $G_\pi = -0.180$ MeV, $G_\nu = -0.131$ MeV, and $\kappa = 0.06$ MeV/r_0^4, the same values as in Ref. [18]. Instead of using assumptions $G^2_\pi = G^2_\nu$ and $\kappa_\pi = \kappa_\nu$, we fix ratios G^2_π/κ_π and G^2_ν/κ_ν for all nuclei.

(ii) Consider nuclei in which there are only valence neutrons. Let us use $p0n1$ to denote nucleus $^{130}_{50}$Sn, in which there are one valence neutron pair but no valence proton pairs (For sake of simplicity, we use in this article pm_1nm_2 to denote nuclei in which there are m_1 valence proton pairs and m_2 valence neutron pairs.). We take $G^2_\nu = -0.013$ MeV/r_0^4, $\kappa_\nu = -0.015$ MeV/r_0^4, the

same values as in Ref. [18] for $^{130}_{50}$Sn nucleus. G_ν^2 and κ_ν with such values well reproduce $E(2_1^+)$ of $^{130}_{50}$Sn. Then we adjust parameters of Hamiltonian for $^{128}_{50}$Sn (i.e., $p0n2$) nucleus. We multiply $G_\nu^2 = -0.013$ and $\kappa_\nu = -0.015$ (parameters for the $p0n1$ case) by a factor α_ν to reproduce $E(2_1^+)$ of $^{128}_{50}$Sn ($p0n2$). Similarly, we obtain parameters for $p0n3$ and $p0n4$ cases.

(iii) We take $G_\pi^2 = -0.025$, $\kappa_\pi = -0.045$ for $^{134}_{52}$Te ($p1n0$). By the same procedure as done for $p0nm_1$ cases, we obtain our parameters for pm_1n0 system.

(iv) For nuclei with m_1 valence proton pairs and m_2 valence neutron pairs, we find factors α_π and α_ν, with the requirements that

$$E(2_1^+)_{\text{cal}} = E(2_1^+)_{\text{exp}} \tag{17}$$

and

$$\frac{E^\pi_{\text{cal}}}{E^\nu_{\text{cal}}} = \frac{E^\pi_{\text{exp}}}{E^\nu_{\text{exp}}}. \tag{18}$$

The E^π_{cal} and E^ν_{cal} denote calculated $E(2_1^+)$ of pm_1n0 case and that of $p0nm_2$ case, respectively, using the parameters of pm_1nm_2. E^π_{exp} and E^ν_{exp} denote experimental data of $E(2_1^+)$ of pm_1n0 case and that of $p0nm_2$ case, respectively. For example, to determine the parameters for the $p4n3$ case, we multiply both $G_\pi^2 = -0.025$ and $\kappa_\pi = -0.045$ by $\alpha_\pi = 1.920$ and multiply $G_\nu^2 = -0.013$, $\kappa_\nu = -0.015$ by $\alpha_\nu = 1.258$. We point out here that the two parameters α_π and α_ν can be uniquely determined by our phenomenological and simple requirements given in Eqs. (17) and (18).

We similarly apply above procedures to these isotopes with valence neutrons in the 82–126 shell. We take $G_\pi = -0.150$ MeV, $G_\nu = -0.131$ MeV, and $\kappa = -0.06$ MeV/r_0^4. Note that κ is negative because both valence protons and valence neutrons are particle-like. For $^{134}_{50}$Sn ($p0n1$) we use $G_\nu^2 = -0.0135$ MeV/r_0^4, $\kappa_\nu = -0.015$ MeV/r_0^4, and for $^{134}_{52}$Te ($p1n0$) we use $G_\pi^2 = -0.0177$ MeV/r_0^4, $\kappa_\pi = -0.032$ MeV/r_0^4. The parameters α_π and α_ν for both shells are listed in Tables II and III.

An argument to adopt the above procedure of determining parameters of our Hamiltonian is presented as follows. Our parametrization is expected to not only reproduce the experimental value of $E(2_1^+)$ but also reflect the relative contribution to $E(2_1^+)$ from protons and neutrons. In principle, one cannot discriminate the contribution from one kind of nucleons from the other because there are proton-neutron correlations. However, we can take into relative contribution into account approximately via the above phenomenological procedure. Along this line the requirement Eq. (18) is found to be important, especially when one discusses $B(E2)$ and $B(M1)$.

In Ref. [18] parameters of the Hamiltonian do not satisfy Eq. (18). If we use those parameters, neutron excited energies will be lower than those in this article and the proton excited energies are higher. So the neutron excitation contribute more to the low-energy states than they should. Reference [18] used nearly equal magnitudes of e_π and e_ν (χ^2-fitting results are $e_\pi = 1.73035e$ and $e_\nu = -1.41201e$). Our χ^2-fitting

TABLE II. α_π and α_ν for nuclei with both valence protons and neutrons in the 50–82 shell (including single-closed shell nuclei). $G_\pi = -0.180$ MeV, $G_\nu = -0.131$ MeV, and $\kappa = 0.06$ MeV/r_0^4 are fixed for all these nuclei. We define $G_\pi^2 = -0.025\alpha_\pi$ MeV/r_0^4, $\kappa_\pi = -0.045\alpha_\pi$ MeV/r_0^4, $G_\nu^2 = -0.013\alpha_\nu$ MeV/r_0^4, $\kappa_\nu = -0.015\alpha_\nu$ MeV/r_0^4. The values of α_π and α_ν are determined by two requirements in Eqs. (17) and (18) for each nucleus.

Nucl.	^{132}Sn	^{130}Sn	^{128}Sn	^{126}Sn	^{124}Sn
α_ν	–	1.000	1.100	1.200	1.230
α_π	–	1.000	1.000	1.000	1.000
Nucl.	^{134}Te	^{132}Te	^{130}Te	^{128}Te	^{126}Te
α_ν	1.000	1.170	1.353	1.512	1.673
α_π	1.000	1.130	1.190	1.250	1.330
Nucl.	^{136}Xe	^{134}Xe	^{132}Xe	^{130}Xe	^{128}Xe
α_ν	1.000	1.320	1.540	1.764	1.980
α_π	0.920	1.113	1.187	1.279	1.371
Nucl.	^{138}Ba	^{136}Ba	^{134}Ba	^{132}Ba	^{130}Ba
α_ν	1.000	1.370	1.573	1.812	2.103
α_π	0.850	1.071	1.131	1.224	1.352
Nucl.	^{140}Ce	^{138}Ce	^{136}Ce	^{134}Ce	^{132}Ce
α_ν	1.000	1.430	1.639	1.920	2.005
α_π	0.850	1.088	1.148	1.258	1.335

TABLE III. α_π and α_ν for nuclei with valence protons in the 50–82 shell but valence neutrons in the 82–126 shell (including single-closed shell nuclei). $G_\pi = -0.150$ MeV, $G_\nu = -0.131$ MeV, $\kappa = -0.06$ MeV/r_0^4 are fixed for all nuclei in this region. We define $G_\pi^2 = -0.0177\alpha_\pi$ MeV/r_0^4, $\kappa_\pi = -0.032\alpha_\pi$ MeV/r_0^4, $G_\nu^2 = -0.0135\alpha_\nu$MeV/$r_0^4$, $\kappa_\nu = -0.015\alpha_\nu$ MeV/r_0^4. α_π and α_ν are determined by Eqs. (17) and (18) for each nucleus.

Nucl.	^{132}Sn	^{134}Sn	^{136}Sn	^{138}Sn	^{140}Sn
α_ν	–	1.000	1.050	1.105	1.140
α_π	–	1.000	1.000	1.000	1.000
Nucl.	^{134}Te	^{136}Te	^{138}Te	^{140}Te	^{142}Te
α_ν	1.000	1.100	1.197	1.249	1.288
α_π	1.000	1.300	1.520	1.540	1.540
Nucl.	^{136}Xe	^{138}Xe	^{140}Xe	^{142}Xe	^{144}Xe
α_ν	1.000	1.100	1.208	1.315	1.368
α_π	0.840	1.134	1.327	1.504	1.588
Nucl.	^{138}Ba	^{140}Ba	^{142}Ba	^{144}Ba	^{146}Ba
α_ν	1.000	1.080	1.197	1.392	1.414
α_π	0.750	0.990	1.208	1.665	1.650
Nucl.	^{140}Ce	^{142}Ce	^{144}Ce	^{146}Ce	^{148}Ce
α_ν	1.000	1.040	1.103	1.216	1.425
α_π	1.020	1.122	1.153	1.295	2.448

calculations give $e_\pi = 1.9389e$, $e_\nu = -1.0795e$, closer to the relation $e_\nu = \delta e$, $e_\pi = (1+\delta)e$ in Ref. [19]. Furthermore, if we used parameters of Ref. [18], our magnetic moment would be much smaller. The details will be presented in next section.

IV. CALCULATED RESULTS

A. Energy spectra

The Hamiltonian (4) is believed to include all the essential ingredients of physics, and it is expected to describe the general features of the low-lying excitations well if the *SD* truncation is good. Our calculated energy spectra of nuclei with valence neutrons in the 50–82 shell are shown in Fig. 1; and results for the 82–126 neutron shell are shown in Fig. 2. In these figures, experimental values are plotted on the left and calculated values on the right. One sees that the low-lying energy levels on low spin states of the ground band and quasi-γ bands are reasonably reproduced, generally speaking. However, we also point out that there are sizable differences between calculated energies of ground-band states and those of experimental data when $I \geq 6$. Such inconsistencies can be improved substantially if one introduces one pair with the largest spin, e.g., pair with spin equal to 10, which is an alignment of two protons in $h_{11/2}$ orbit (see Ref. [9]). In this article we are interested in only very low spin states and thus such configurations are not taken into account.

B. $B(E2)$ values

To describe the experimental data of $E2$ transition rates, we perform the χ^2 fitting of $B(E2, 0_1^+ \to 2_1^+)$ to obtain our effective charges, e_π and e_ν. We get $e_\pi = 1.9389e$ and $e_\nu = -1.0795e$ for nuclei with valence neutrons in the 50–82 shell and $e_\pi = 1.9389e$ and $e_\nu = 1.0795e$ for those with valence neutrons in the 82–126 shell. e_ν has a minus sign in the neutron 50–82 shell because valence neutrons are holelike in this case. Note that these e_π and e_ν values are consistent approximately with relation $e_\nu = \delta e$ and $e_\pi = (1+\delta)e$ in Ref. [19]. The calculated $B(E2, 0_1^+ \to 2_1^+)$ values are listed in "cal1" of Table IV. In Ref. [18], $e_\pi = 1.73035e$, $e_\nu = -1.41201e$ for the neutron 50–82 shell. Their absolute values are nearly equal. The reason is that Hamiltonian parameters of Ref. [18] lead to larger contributions from valence neutrons. Correspondingly, a larger value of e_ν is necessary to reproduce experimental data.

It is also interesting to perform the χ^2 fitting of $B(E2)$ for nuclei with valence neutrons in the 50–82 shell and for

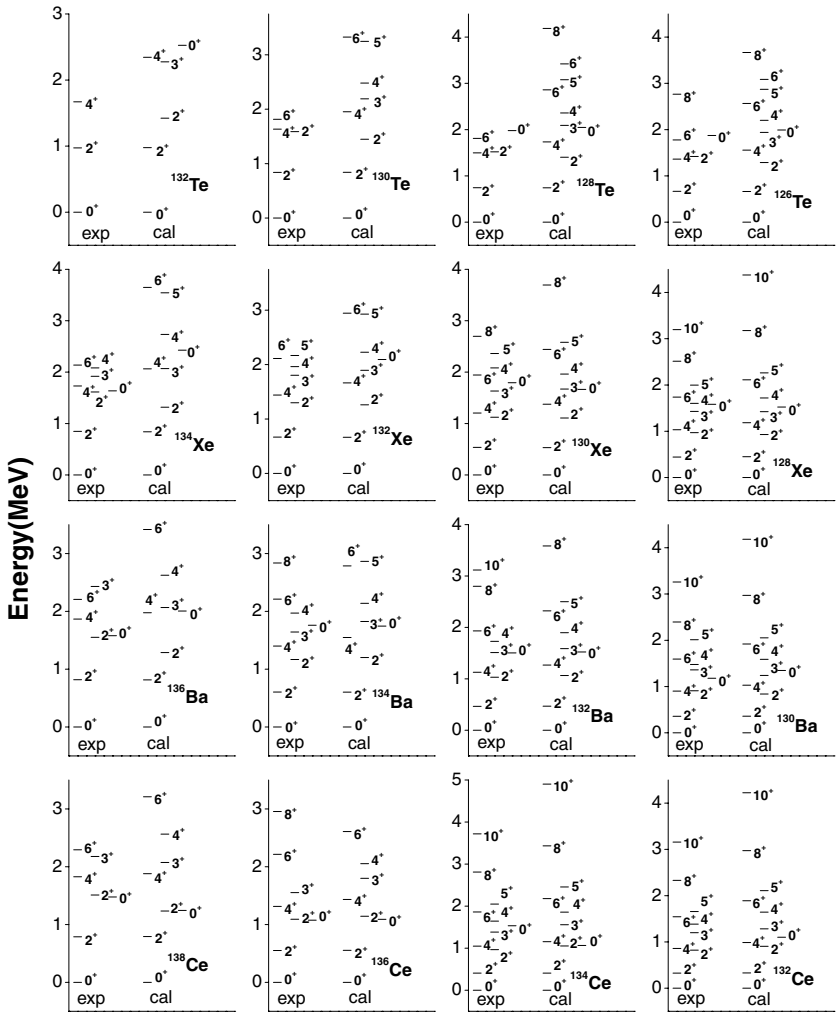

FIG. 1. The energy spectra of nuclei with both valence protons and neutrons in the 50–82 shell. The left-hand side of each figure is plotted based on the experimental data, which are taken from Ref. [17], whereas the right-hand side is plotted based on our calculated results.

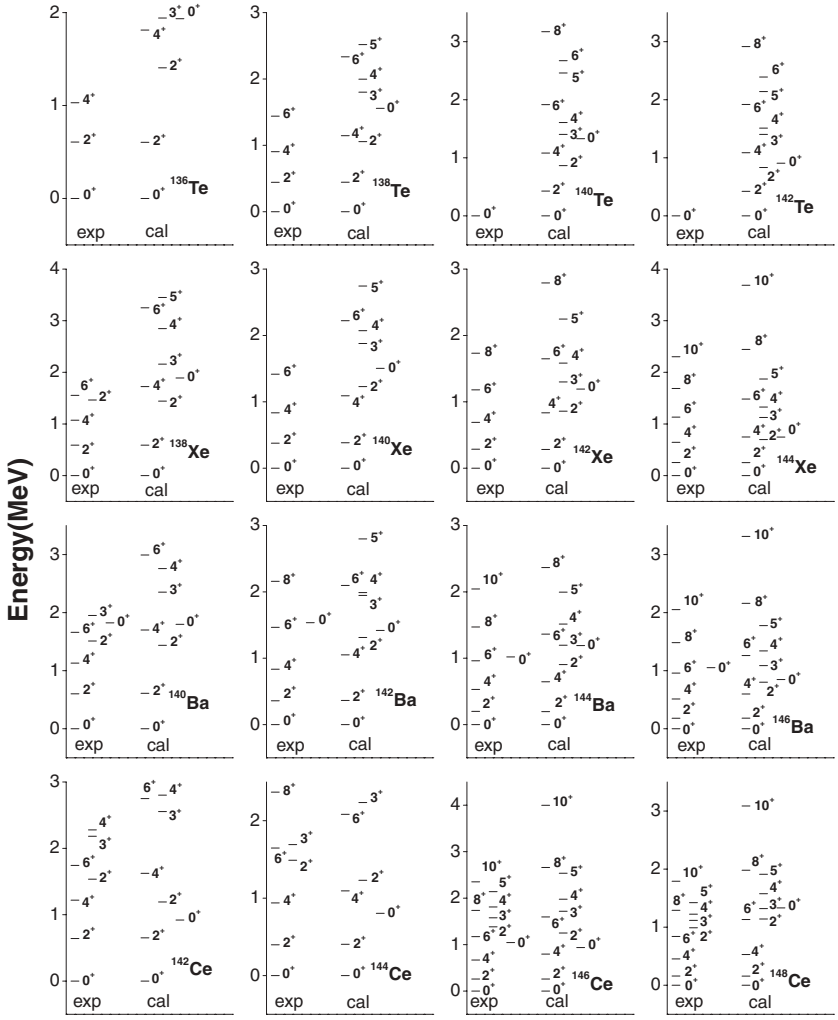

FIG. 2. Same as described in the legend to Fig. 1 except for nuclei with valence protons in the 50–82 shell and valence neutrons in the 82–126 shell.

those with valence neutrons in the 82–126 shell separately. We obtain $e_\pi = 1.91e$ and $e_\nu = -1.17e$ for the former case and $e_\pi = 1.93e$ and $e_\nu = 1.04e$ for the latter. Both sets are close to each other and to above results ($e_\pi = 1.9389e$ and $e_\nu = 1.0795e$), which are obtained by χ^2-fitting of $B(E2)$ for all nuclei in this article.

One sees that our such calculated $B(E2, 0_1^+ \to 2_1^+)$ are larger than the experimental data near the closed shell, and smaller far from the closed shell. To get a better fit with the experimental data, we take effective charges which are linear with valence pair number of the nuclei, introduced empirically in Ref. [20]. We use $e_\pi = (1+\delta)e$. $e_\nu = -\delta e$ in the neutron 50–82 shell, and $e_\nu = \delta e$ in the neutron 82–126 shell. In Ref. [20], Yoshinaga and Higashiyama used $\delta = 0.6 + 0.05(N_\pi + N_\nu)$. N_π and N_ν are pair numbers of valence protons and valence neutrons, respectively. We used $\delta = 0.577 + 0.0781(N_\pi + N_\nu)$, in which coefficients 0.577, 0.0781 are obtained via the χ^2-fitting procedure. By using these effective charges, the agreement with the experimental data is improved. Our calculated results of $B(E2)$ values are presented in "cal2" of Table IV.

Recent experimental data of $B(E2)$ values for $^{132-136}$Te attracted much interest, because they are very much hindered. There have been a number of shell-model calculations to describe these results [10,18]. We can reasonably describe these $B(E2)$ values if we fix our effective charges. The description can be improved if our effective charges increases with number of valence pairs very slowly, as shown in Table IV.

In Table IV we also present our calculated results of $B(E2)$ for $^{126-140}$Sn and $^{138-142}$Te for which no experimental data of $B(E2)$ are available, and $^{138-144}$Xe for which experimental data are incomplete. We hope that some of them will be measured in near future.

In many previous calculations [9,20,21] of above nuclei with valence neutrons in the 50–82 shell, relative $B(E2)$ values were calculated and compared with experimental data. Some of these nuclei exhibit nearly O(6) behavior of the interacting boson model. Our calculations are consistent with those results in this respect, as shown in Table V.

C. *g* factor

We have also calculated $g_{2_1^+}$. Because experimental data are very scarce (especially for nuclei within the neutron 82–126 shell), we did not perform the χ^2-fitting procedure. We take $g_{l\pi} = 1\mu_N$ and $g_{l\nu} = 0$ throughout this article. In "cal1" of Table VI we use $g_{s\pi} = 5.586 \times 0.7\mu_N$, $g_{s\nu} = -3.826 \times 0.7\mu_N$, i.e., free nucleon g factors multiplied by a factor

TABLE IV. The $B(E2, 0_1^+ \to 2_1^+)$ in unit e^2b^2. The left side of this table corresponds to the case with valence neutrons in the 50–82 shell, whereas the right side corresponds to the case with valence neutrons in the 82–126 shell. Nuclei without valence neutrons are listed twice, the first is based on parameters given in Table II and the second is based on those in Table III. We present here two sets of results, denoted by "cal1" and "cal2," respectively. In "cal1" effective charges $e_\pi = 1.9389e$ and $|e_\nu| = 1.0795e$ (e_ν takes minus sign for valence neutrons in the 50–82 shell and positive sign for valence neutrons in the 82–126 shell) are fixed; in "cal2" e_π and e_ν change linearly with total pair number of valence neutrons and valence protons. These effective charges in "cal1" are obtained by χ^2 fitting of the experimental data for $B(E2)$ in both shells. To describe effective charges used in "cal2," we define $e_\pi = (1+\delta)e$. $e_\nu = -\delta e$ for nuclei with valence neutrons in the 50–82 shell, and $e_\nu = \delta e$ for those with valence neutrons in the 82–126 shell. δ change with the relation $\delta = 0.577 + 0.0781\,(N_\pi + N_\nu)$. N_π and N_ν are the pair numbers of the valence protons, valence neutrons respectively. The two coefficients 0.577 and 0.0781 in δ are obtained via the χ^2 fitting. These two coefficients are very close to those taken in Ref. [20], where $\delta = 0.6 + 0.05\,(N_\pi + N_\nu)$. The experimental data are taken from Refs. [22,39].

Nucl.	^{124}Sn	^{126}Sn	^{128}Sn	^{130}Sn	^{132}Sn	^{132}Sn	^{134}Sn	^{136}Sn	^{138}Sn	^{140}Sn
Cal1	0.1922	0.1653	0.1244	0.0699	–	–	0.0969	0.1680	0.2130	0.2401
Cal2	0.1305	0.0934	0.0574	0.0257	–	–	0.0357	0.0775	0.1203	0.1630
Exp.	0.1660(40)	–	–	–	–	–	–	–	–	–
Nucl.	^{126}Te	^{128}Te	^{130}Te	^{132}Te	^{134}Te	^{134}Te	^{136}Te	^{138}Te	^{140}Te	^{142}Te
Cal1	0.4638	0.4155	0.3479	0.2616	0.1743	0.1694	0.2667	0.4049	0.4981	0.5501
Cal2	0.4115	0.3267	0.2444	0.1697	0.1270	0.1234	0.1598	0.2717	0.3802	0.4777
Exp.	0.475(10)	0.383(6)	0.295(7)	0.172(17)	0.096(12)	0.096(12)	0.103	–	–	–
Nucl.	^{128}Xe	^{130}Xe	^{132}Xe	^{134}Xe	^{136}Xe	^{136}Xe	^{138}Xe	^{140}Xe	^{142}Xe	^{144}Xe
Cal1	0.7029	0.6278	0.5260	0.4023	0.2763	0.2515	0.4156	0.6239	0.7803	0.9172
Cal2	0.7218	0.5802	0.4397	0.3106	0.2208	0.2010	0.3054	0.5045	0.7045	0.9265
Exp.	0.750(40)	0.65(5)	0.460(30)	0.34(6)	0.36(6)	0.36(6)	–	0.324(14)	–	–
Nucl.	^{130}Ba	^{132}Ba	^{134}Ba	^{136}Ba	^{138}Ba	^{138}Ba	^{140}Ba	^{142}Ba	^{144}Ba	^{146}Ba
Cal1	0.8814	0.7774	0.6430	0.4760	0.3212	0.2579	0.4581	0.7455	1.0078	1.1959
Cal2	1.0155	0.8117	0.6098	0.4144	0.2803	0.2250	0.3829	0.6890	1.0342	1.3606
Exp.	1.163(16)	0.86(6)	0.658(7)	0.410(8)	0.230(9)	0.230(9)	0.45(19)	0.699(37)	1.05(6)	1.355(48)
Nucl.	^{132}Ce	^{134}Ce	^{136}Ce	^{138}Ce	^{140}Ce	^{140}Ce	^{142}Ce	^{144}Ce	^{146}Ce	^{148}Ce
Cal1	1.0989	0.9689	0.7691	0.5273	0.3427	0.1918	0.4520	0.8980	1.2884	1.6447
Cal2	1.3981	1.1249	0.8142	0.5100	0.3255	0.1822	0.4231	0.9363	1.4822	2.0827
Exp.	1.87(17)	1.04(9)	0.81(9)	0.450(30)	0.298(6)	0.298(6)	0.480(6)	0.83(9)	1.14(12)	1.96(18)

TABLE V. The relative $B(E2)$ values of ^{130,132,134}Ba and ^{128,130}Xe. The experimental data are taken from Ref. [32]. "O(6)" means the relative $B(E2)$ transitions of the IBM prediction in the O(6) limit. $e_\pi = 1.9389e$, and $e_\nu = -1.0795e$. One sees that our calculations reasonably reproduce the O(6) behavior for these nuclei.

Nucl. $J_i \to J_f$	O(6)	^{132}Ba		^{134}Ba		^{130}Xe		^{130}Ba		^{128}Xe	
		Exp.	Cal.	Exp.	Cal.	Exp.	Cal.	Exp.	Cal.	Exp.	Cal.
$2_2^+ \to 2_1^+$	100	100	100	100	100	100	100	100	100	100	100
$\to 0_1^+$	0	0.2	1.34	0.6	0.05	8	0.0646	5.7	2.64	1.2	0.05
$3_1^+ \to 2_2^+$	100	100	100	100	100	100	100	100	100	100	100
$\to 4_1^+$	40	73	28.1	40	29.4	25	30.2	30	32.5	37	35.5
$\to 2_1^+$	0	0.2	0.601	1.0	0.0153	1.4	0.055	1.5	1.45	1	0.02
$4_2^+ \to 2_2^+$	100	100	100	100	100	100	100	100	100	100	100
$\to 3_1^+$	0	–	9.32	14.5	5.07	–	0.005	–	9.54	–	0.401
$\to 4_1^+$	91	75	59.8	77	58.9	107	93.9	89	61.6	133	102
$\to 2_1^+$	0	2.2	2.12	2.5	5.38	3.2	5.06	3.9	2.01	1.7	4.64
$5_1^+ \to 3_1^+$	100	100	100	100	100	100	100	100	100	100	100
$\to 4_2^+$	46	–	84.0	–	88.7	–	106	$\leqslant$57	86.0	88	99.3
$\to 6_1^+$	45	–	50.7	–	55.7	–	61.1	381	56.8	204	61.7
$\to 4_1^+$	0	–	0.526	–	1.81	–	4.36	6.7	0.142	3.7	3.60
$0_2^+ \to 2_2^+$	100	100	100	100	100	100	100	100	100	100	100
$\to 2_1^+$	0	0	45.3	4	77.2	2.6	19.0	–	14.4	14	4.07

TABLE VI. g factor of 2_1^+ state (in unit of μ_N). The left side of this table is for the neutron 50–82 shell, whereas the right side is for the neutron 82–126 shell. Nuclei without valence neutrons are calculated twice by using two sets of parameters given in Tables II and III. We fix $g_{l\pi} = 1\mu_N$, $g_{l\nu} = 0$ throughout this article but take two sets of $g_{s\nu}$ and $g_{s\pi}$: $g_{s\pi} = 5.586 \times 0.7\mu_N$, $g_{s\nu} = -3.826 \times 0.7\mu_N$ in the first set (denoted by "cal1") and $g_{s\pi} = 5.586\mu_N$, $g_{s\nu} = -3.826\mu_N$ in the second set (denoted by "cal2"). In case that there is a big difference between several sets of experimental data, we list both the largest and the smallest, denoted by "exp1" and "exp2," otherwise we present the experimental data in "exp1." SM1 and SM2 are two sets of shell-model-calculated results. SM1 is from Ref. [11], SM2 is from Ref. [12].

Nucl.	^{124}Sn	^{126}Sn	^{128}Sn	^{130}Sn	^{132}Sn	^{132}Sn	^{134}Sn	^{136}Sn	^{138}Sn	^{140}Sn
Cal1	−0.111	−0.106	−0.101	−0.096	–	–	−0.036	−0.039	−0.040	−0.038
Cal2	−0.159	−0.151	−0.144	−0.137	–	–	−0.051	−0.055	−0.057	−0.054
Exp1	−0.15(10)[a]	–	–	–	–	–	–	–	–	–
SM2	−0.125	−0.120	−0.115	−0.126	–	–	−0.221	–	–	–
Nucl.	^{126}Te	^{128}Te	^{130}Te	^{132}Te	^{134}Te	^{134}Te	^{136}Te	^{138}Te	^{140}Te	^{142}Te
Cal1	0.163	0.192	0.241	0.337	0.879	0.860	0.148	0.121	0.100	0.081
Cal2	0.110	0.139	0.188	0.283	0.809	0.780	0.119	0.093	0.072	0.055
Exp1	0.31(4)[b]	0.25(3)[b]	0.29(5)[b]	0.35(5)[c]	–	–	–	–	–	–
Exp2	0.19(3)[d]	0.35(4)[e]	–	–	–	–	–	–	–	–
SM1	–	–	0.598	0.648	0.811	0.811	–	–	–	–
SM2	–	–	0.341	0.479	0.833	0.833	0.348	–	–	–
Nucl.	^{128}Xe	^{130}Xe	^{132}Xe	^{134}Xe	^{136}Xe	^{136}Xe	^{138}Xe	^{140}Xe	^{142}Xe	^{144}Xe
Cal1	0.293	0.325	0.369	0.456	0.881	0.855	0.272	0.223	0.181	0.156
Cal2	0.239	0.271	0.314	0.400	0.813	0.771	0.233	0.187	0.147	0.123
Exp1	0.31(3)[f]	–	0.349(34)[g]	0.504(49)[g]	0.83(10)[g]	0.83(10)[g]	–	–	–	–
Exp2	0.41(7)[h]	0.334(11)[i]	0.314(12)[i]	0.354(7)[i]	0.766(45)[i]	0.766(45)[i]	–	–	–	–
SM1	–	–	0.510	0.594	0.812	0.812	–	–	–	–
SM2	–	–	–	0.412	0.884	0.884	0.394	–	–	–
Nucl.	^{130}Ba	^{132}Ba	^{134}Ba	^{136}Ba	^{138}Ba	^{138}Ba	^{140}Ba	^{142}Ba	^{144}Ba	^{146}Ba
Cal1	0.403	0.415	0.447	0.486	0.909	0.875	0.297	0.297	0.253	0.216
Cal2	0.352	0.365	0.397	0.438	0.857	0.803	0.262	0.258	0.215	0.180
Exp1	0.35(3)[j]	0.34(3)[j]	0.43(5)[j]	0.345(50)[j]	0.7(1)[k]	0.7(1)[k]	–	0.425(50)[l]	0.34(5)[m]	0.28(7)[m]
SM2	–	–	–	–	0.98	0.98	–	–	–	–
Nucl.	^{132}Ce	^{134}Ce	^{136}Ce	^{138}Ce	^{140}Ce	^{140}Ce	^{142}Ce	^{144}Ce	^{146}Ce	^{148}Ce
Cal1	0.514	0.521	0.532	0.514	0.977	0.980	0.350	0.432	0.400	0.336
Cal2	0.475	0.484	0.498	0.484	0.964	0.968	0.331	0.405	0.370	0.304
Exp1	–	–	–	–	0.95(10)[n]	0.95(10)[n]	0.21(5)[n]	–	0.24(5)[o]	0.37(6)[o]

Experimental data:
[a]Experimental data from Ref. [25]
[b]Experimental data from Ref. [26]
[c]Experimental data from Ref. [27]
[d]Experimental data from Ref. [28]
[e]Experimental data from Ref. [29]
[f]Experimental data from Ref. [30]
[g]Experimental data from Ref. [31]
[h]Experimental data from Ref. [33]
[i]Experimental data from Ref. [11]
[j]Experimental data from Ref. [34]
[k]Experimental data from Ref. [35]
[l]Experimental data from Ref. [36]
[m]Experimental data from Ref. [37]
[n]Experimental data from Ref. [23]
[o]Experimental data from Ref. [38]

of 0.7. In "cal2" of Table VI we use $g_{s\pi} = 5.586\mu_N$, $g_{s\nu} = -3.826\mu_N$, which are g factors of a free proton and a free neutron, respectively.

The calculated $g_{2_1^+}$ are listed in Table VI. The tendency of our calculated $g_{2_1^+}$ is consistent in general with the formula $g(2_1^+) = \frac{N_\pi}{N_\pi + N_\nu}$ suggested in Ref. [24], which predicted that $g_{2_1^+}$ increase with N_π and decrease with N_ν, although there are also a few exceptions in our calculated results that violate such a tendency. We also list two sets of results using a shell model for comparison. One sees from Table VI that both sets of our calculations describe the experimental data very well, although we do not adjust g factors in transition operators. Therefore, we present our calculated results of $g_{2_1^+}$ for all nuclei discussed in this article and hope that our predicted results are useful to future measurements of $g_{2_1^+}$ for nuclei in this region.

We note that $g_{2_1^+}$ values calculated by using parameters in Ref. [18] are not in good agreement with experimental data.

V. DISCUSSION AND SUMMARY

In this article we introduce a new procedure to find parameters of the phenomenological shell-model Hamiltonian that consists of single particle energies, monopole and quadrupole pairing interactions, and quadrupole-quadrupole interactions between valence protons, valence neutrons, and valence protons and valence neutrons. We apply this phenomenological Hamiltonian and nucleon pair approximation of the shell model to Sn, Te, Xe, Ba, and Ce isotopes with mass number $A \sim 120$–150 and neutron number ranging from 74 to 90. The parameters in our Hamiltonian for cases with both valence protons and valence neutrons outside the core are determined by experimental data of $E_{2_1^+}$ and our phenomenological requirements introduced in this article. To achieve this, one needs only strengths of monopole pairing, neutron-proton interaction, and parametrization of three single-closed nuclei, Sn^{134}, Te^{130}, and Te^{134}. In previous calculations, one may get similar outputs even if one takes different sets of parameters with sizable differences, whereas here we remove such ambiguities by using our phenomenological requirements.

Our nucleon pairs are restricted to correlated S and D pairs. We take the BCS pair as our S pair and D pair is obtained by commutating quadrupole operator Q with the S pair. By choosing such SD-pair subspace, we diagonalize the shell-model Hamiltonian and study low-lying states of Sn, Te, Xe, Ba, and Ce isotopes with neutron numbers ranging from 74 to 90. Our calculated results well reproduce the eigenenergies of low-lying states. Our systematic calculations also describe reasonably $B(E2)$ values and $g_{2_1^+}$ for these nuclei in cases where experimental data are available.

Recent development of the radioactive beam facilities provides us with opportunities to explore the nuclear structure of new regions of the nuclear chart. Many new and interesting data of nuclear structure become available, some of which challenge previous calculations. For example, the anomaly of $B(E2, 0_1^+ \to 2_1^+)$ for ^{136}Te [39] has attracted much attention. The $B(E2)$ value for this nucleus is exceptionally hindered (a similar situation occurs in nucleus ^{16}C; see Ref. [40]). In this article we also calculated and discussed $B(E2)$ values of Te isotopes in the neutron-rich side, including the ^{136}Te nucleus. Our pair approximation can reproduce the experimental result of Ref. [39] by taking effective charges that increase very slowly with the number of pairs.

In previous works, systematic calculations of nuclei in this region concentrated on neutron deficient side for Sn, Te, Xe, Ba, and Ce isotopes. For the neutron-rich side, further experimental measurements and theoretical calculations are warranted. Encouraged by the success of applying the SD pair approximations to nuclei with relatively rich data, we also present in this article predicted results of $B(E2)$ values and g factors for nuclei without experimental measurements (in particular, Sn, Te, and Xe isotopes). We expect with the updated radioactive beam facilities measurement of these quantities can be performed in the near future.

ACKNOWLEDGMENTS

Communication with Professor N. Yoshinaga is gratefully acknowledged. One of the authors (Y.M.Z.) thanks the National Natural Science Foundation of China for supporting this work under grants 10545001, 10575070, and 10675081. This work is also supported partly by the PRP program of Shanghai Jiao Tong University, the Research Foundation for Doctoral Program of Higher Education of China under grant No. 20060248050, and Scientific Research Foundation of Ministry of Education in China for Returned Scholars.

[1] A. Arima and F. Iachello, Ann. Phys. **99**, 253 (1976); **111**, 209 (1978); **123**, 468 (1979); for a review, see F. Iachello and A. Arima, *The Interacting Boson Model* (Cambridge University Press, Cambridge, 1987).
[2] C. L. Wu, D. H. Feng, X. G. Chen, J. Q. Chen, and M. Guidry, Phys. Rev. C **36**, 1157 (1987).
[3] Y. K. Gambir, S. Haq, and J. K. Suri, Ann. Phys. (NY) **133**, 154 (1981).
[4] K. T. Hecht, J. B. McGrory, and J. P. Draayer, Nucl. Phys. **A197**, 369 (1972).
[5] J. Q. Chen, B. Q. Chen, and A. Klein, Nucl. Phys. **A554**, 61 (1993); **A562**, 218 (1993).
[6] J. Q. Chen, Nucl. Phys. **A626**, 686 (1997).
[7] Y. M. Zhao, N. Yoshinaga, S. Yamaji, J. Q. Chen, and A. Arima, Phys. Rev. C **62**, 014304 (2000).
[8] N. Yoshinaga, T. Mizusaki, A. Arima, and Y. D. Devy, Prog. Theor. Phys. **125** (suppl.), 65 (1996).
[9] K. Higashiyama, N. Yoshinaga, and K. Tanabe, Phys. Rev. C **67**, 044305 (2003).
[10] N. Shimizu, T. Otsuka, T. Mizusaki, and M. Honma, Phys. Rev. C **70**, 054313 (2004).
[11] G. Jakob, N. Benczer-Koller, G. Kumbartzki, J. Holden, T. J. Mertzimekis, K.-H. Speidel, R. Ernst, A. E. Stuchbery, A. Pakou, P. Maier-Komor, A. Macchiavelli, M. McMahan,

L. Phair, and I. Y. Lee, Phys. Rev. C **65**, 024316 (2002).
[12] B. A. Brown, N. J. Stone, J. R. Stone, I. S. Towner, and M. Hjorth-Jensen, Phys. Rev. C **71**, 044317 (2005).
[13] S. Yoshida, Phys. Rev. **123**, 2122 (1961).
[14] K. Allart, E. Boeker, G. Bonsignori, M. Saroia, and Y. K. Gambhir, Phys. Rep. **169**, 209 (1988); I. Talmi, Nucl. Phys. **A172**, 1 (1972).
[15] B. Fogelberg and J. Blomqvist, Nucl. Phys. **A429**, 205 (1984).
[16] W. J. Baldridge, Phys. Rev. C **18**, 530 (1978).
[17] ENSDF Viewer, National Nuclear Data Center, http://ie.lbl.gov/ensdf/
[18] Y. M. Zhao, S. Yamaji, N. Yoshinaga, and A. Arima, Phys. Rev. C **62**, 014315 (2000); Y. M. Zhao, N. Yoshinaga, S. Yamaji, and A. Arima, *ibid*. **62**, 024322 (2000).
[19] A. Bohr and B. Mottelson, *Nuclear Structure* (Benjamin, New York, 1975), Vol. 1.
[20] N. Yoshinaga and K. Higashiyama, Phys. Rev. C **69**, 054309 (2004).
[21] Y. A. Luo and J. Q. Chen, Phys. Rev. C **58**, 589 (1998); Y. A. Luo, J. Q. Chen, and J. P. Draayer, Nucl. Phys. **A669**, 101 (2000).
[22] S. Raman, C. W. Nestor, Jr., and P. Tikkanen, At. Data Nucl. Data Tables **78**, 1 (2001).
[23] N. J. Stone, Table of Nuclear Magnetic Dipole and Electric Quadrupole Moments, 2001, preprint, Oxford University, United Kingdom.
[24] T. J. Mertzimekis, A. E. Stuchbery, N. Benczer-Koller, and M. J. Taylor, Phys. Rev. C **68**, 054304 (2003).
[25] M. Hass, C. Broude, Y. Niv, and A. Zemel, Phys. Rev. C **22**, 97 (1980).
[26] J. S. Dunham, R. T. Westervelt, R. Avida, and S. S. Hanna, Phys. Rev. C **37**, 2881 (1988).
[27] N. J. Stone, A. E. Stuchbery, M. Danchev, J. Pavan, C. L. Timlin, C. Baktash, C. Barton, J. R. Beene, N. Benczer-Koller, C. R. Bingham, J. Dupak, A. Galindo-Uribarri, C. J. Gross, G. Kumbartzki, D. C. Radford, J. R. Stone, and N. V. Zamfir, Phys. Rev. Lett. **94**, 192501 (2005).
[28] N. K. B. Shu, R. Levy, N. Tsoupas, A. Lopez-Garcia, W. Andrejtscheff, and N. Benczer-Koller, Phys. Rev. C **24**, 954 (1981).
[29] A. Aprahamian, D. S. Brenner, R. F. Casten, R. L. Gill, and A. Piotrowski, Bull. Am. Phys. Soc. **30**, 1264 (1985).
[30] D. M. Gordon, L. S. Eytel, H. de Waard, and D. E. Murnick, Phys. Rev. C **12**, 628 (1975).
[31] K. -H. Speidel, H. Busch, S. Kremeyer, U. Knopp, J. Cub, M. Bussas, W. Karle, K. Freitag, U. Grabowy, and J. Gerber, Nucl. Phys. **A552**, 140 (1993).
[32] R. F. Casten and P. Von Brentano, Phys. Lett. **B152**, 22 (1985).
[33] A. Arnesen, K. Johansson, E. Karlsson, T. Noreland, L.-O. Norlin, and S. Ogaza, Hyperfine Interact. **5**, 81 (1997).
[34] J. M. Brennan, M. Hass, N. K. B. Shu, and N. Benczer-Koller, Phys. Rev. C **21**, 574 (1980).
[35] D. Bazzacco, F. Brandolini, K. Ltiwenich, P. Pavan, and C. Rossi-Alvarez, Z. Phys. A **328**, 275 (1987).
[36] A. Wolf, R. L. Gill, H. Mach, R. F. Casten, and J. A. Winger, Phys. Rev. C **37**, 1253 (1988).
[37] A. Wolf, Z. Berant, D. D. Warner, R. L. Gill, M. Schmid, R. E. Chrien, G. F. Peaslee, H. Yamamoto, J. C. Hill, F. K. Wohn, C. Chung, and W. B. Walters, Phys. Lett. **B123**, 165 (1983).
[38] R. L. Gill, D. D. Warner, H. Mach, A. Piotrowski, A. Wolf, John C. Hill, F. K. Wohn, J. A. Winger, and B. Fogelberg, Phys. Rev. C **33**, 1030 (1986).
[39] D. C. Radford, C. Baktash, J. R. Beene, B. Fuentes, A. Galindo-Uribarri, C. J. Gross, P. A. Hausladen, T. A. Lewis, P. E. Mueller, E. Padilla, D. Shapira, D. W. Stracener, C.-H. Yu, C. J. Barton, M. A. Caprio, L. Coraggio, A. Covello, A. Gargano, D. J. Hartley, and N. V. Zamfir, Phys. Rev. Lett. **88**, 0222501 (2002).
[40] N. Imai, H. J. Ong, N. Aoi, H. Sakurai, K. Demichi, H. Kawasaki, H. Baba, Zs. Dombradi, Z. Elekes, N. Fukuda, Zs. Fueloep, A. Gelberg, T. Gomi, H. Hasegawa, K. Ishikawa, H. Iwasaki, E. Kaneko, S. Kanno, T. Kishida, Y. Kondo, T. Kubo, K. Kurita, S. Michimasa, T. Minemura, M. Miura, T. Motobayashi, T. Nakamura, M. Notani, T. K. Onishi, A. Saito, S. Shimoura, T. Sugimoto, M. K. Suzuki, E. Takeshita, S. Takeuchi, M. Tamaki, K. Yamada, K. Yoneda, H. Watanabe, and M. Ishihara, Phys. Rev. Lett. **92**, 222501 (2004).